

Waveform Integrity in Atrial Fibrillation: The Forgotten Issue of Cardiac Electrophysiology

MIGUEL MARTÍNEZ-INIESTA,¹ JUAN RÓDENAS,¹ RAÚL ALCARAZ,¹ and JOSÉ J. RIETA²

¹Research Group in Electronic, Biomedical and Telecommunication Engineering, University of Castilla-La Mancha, Albacete, Spain; and ²BioMIT.org, Electronic Engineering Department, Universidad Politécnica de Valencia, Valencia, Spain

(Received 28 October 2016; accepted 5 April 2017; published online 18 April 2017)

Associate Editor Ender A Finol oversaw the review of this article.

Abstract—Atrial fibrillation (AF) is the most common arrhythmia in clinical practice with an increasing prevalence of about 15% in the elderly. Despite other alternatives, catheter ablation is currently considered as the first-line therapy for the treatment of AF. This strategy relies on cardiac electrophysiology systems, which use intracardiac electrograms (EGM) as the basis to determine the cardiac structures contributing to sustain the arrhythmia. However, the noise-free acquisition of these recordings is impossible and they are often contaminated by different perturbations. Although suppression of nuisance signals without affecting the original EGM pattern is essential for any other later analysis, not much attention has been paid to this issue, being frequently considered as trivial. The present work introduces the first thorough study on the significant fallout that regular filtering, aimed at reducing acquisition noise, provokes on EGM pattern morphology. This approach has been compared with more refined denoising strategies. Performance has been assessed both in time and frequency by well established parameters for EGM characterization. The study comprised synthesized and real EGMs with unipolar and bipolar recordings. Results reported that regular filtering altered substantially atrial waveform morphology and was unable to remove moderate amounts of noise, thus turning time and spectral characterization of the EGM notably inaccurate. Methods based on Wavelet transform provided the highest ability to preserve EGM morphology with improvements between 20 and beyond 40%, to minimize dominant atrial frequency estimation error with up to 25% reduction, as well as to reduce huge levels of noise with up to 10 dB better reduction. Consequently, these algorithms are recommended as a replacement of regular filtering to avoid significant alterations in the EGMs. This could lead to more accurate and truthful analyses of atrial activity dynamics aimed at understanding and locating the sources of AF.

Keywords—Atrial fibrillation, Electrogram, Filtering, Wavelet transform, Empirical mode decomposition.

INTRODUCTION

Atrial fibrillation (AF) is currently one of the major cardiovascular challenges in the developed world.⁴⁴ It is the most common supra-ventricular arrhythmia in clinical practice, affecting approximately 1.5–2% of the general population.⁶⁰ More than 33 million individuals worldwide have AF, and 5 million of new cases are approximately diagnosed each year.¹² Moreover, its incidence and prevalence increase with age, thus around 15% of people older than 80 years suffer from this arrhythmia.⁶⁰ However, the reasons for the increasing impact of AF on aged population⁴⁹ as well as the underlying electrophysiological mechanisms of this arrhythmia⁵⁰ are still topics of intense discussion due to their incomplete understanding. Indeed, this aspect hampers effective diagnosis and treatment of the arrhythmia, thus causing that 15% of the healthcare budget in cardiac diseases has to be spent on the management of AF.⁵⁷

Within this context, the analysis of atrial electrical activity is of paramount relevance to improve current knowledge on the mechanisms responsible for initiation, maintenance and perpetuation of AF.²³ This information can be analyzed either from surface recordings, i.e., from the electrocardiogram (ECG),^{3,22} or from intracardiac recordings, i.e., from electrograms (EGM).²⁴ Whereas the ECG records the superposition of the heart's electrical activity from the patient's thorax, the EGM directly captures local electrical activity on the cardiac tissue. Therefore, this latter recording provides more detailed information about the electrical status of any particular area of the

Address correspondence to Miguel Martínez-Iniesta, Research Group in Electronic, Biomedical and Telecommunication Engineering, University of Castilla-La Mancha, Albacete, Spain. Electronic mail: miguel.martinez@uclm.es

myocardium than the ECG, thus being nowadays the hallmark of cardiac electrophysiology.¹⁵ In fact, the EGM can provide accurate information about the time, direction and complexity of atrial activations within the field of view of the recording electrodes.²⁶ As a result of this near-field information, current cardiac mapping systems are able to provide nonfluoroscopic electroanatomic maps which help in determining the site of arrhythmia origin, its mechanism as well as the particular cardiac structures sustaining AF.²⁹ Knowledge of the arrhythmia mechanism and circuit is critical in planning arrhythmia ablation, which is currently considered as the first-line therapy for the treatment of AF.³⁵

Every single EGM responds to the potential differences recorded at two separated electrodes. In this regard, two different signals are widely used in clinical electrophysiology, namely unipolar and bipolar recordings.⁵³ Unipolar EGMs are obtained by placing an electrode in the heart's surface and the second one distant from it to serve as a reference. This recording provides information about the impulse propagation direction, but substantial far-field signals, generated by depolarization of remote tissues, are also acquired.⁵³ On the contrary, bipolar EGMs are obtained by attaching closely two electrodes in a specific area of the cardiac tissue, thus mostly providing information about local electrical activity.⁵³ The main disadvantage of this recording is the impossibility of quantifying wavefront propagation direction.²⁶ Hence, both types of recordings contain complementary information and, usually, both are simultaneously acquired to assist cardiac mapping techniques.²⁶

Although to a lesser extent than for the surface ECG, noise and other nuisance signals also disturb EGM acquisition.⁵⁵ From an electromagnetical point of view, the electrophysiology laboratory is an extraordinarily noisy environment,⁵⁵ where a wide conglomerate of electrical equipments, some of them connected to the patient's body, are simultaneously operating. These equipments provoke high-frequency and broadband noises, which are unavoidably recorded during EGM acquisition.⁵⁵ Another important source of interference is the electrical mains, which often contaminates EGM recordings with a component of 50 or 60 Hz.⁵⁶ Finally, the EGM can also be corrupted by high-frequency noise generated from non-cardiac muscle activity of the patient as well as by a low-frequency component, such as the baseline wander, resulting from respiratory or catheter movements and an unstable catheter contact.⁵⁶

Considering that a signal-to-noise ratio (SNR) of 20 dB has been proposed as a recommended minimum

recording quality to discern small changes in any EGM,⁵⁵ the application of an adequate preprocessing method able to reduce noise and preserve waveform pattern is of paramount relevance for successful and reliable further analysis.³⁸ However, this aspect has been the forgotten issue of cardiac electrophysiology studies, with very reduced attention in the literature, thus lacking of thorough validation analysis.³⁸ In fact, the EGM is regularly filtered during its acquisition to reduce power-line interference, far-field signals as well as low- and high-frequency noises, but no alternative preprocessing is often considered.^{37,41} Most of the time, a filtering-based strategy, proposed by Botteron and Smith more than 20 years ago,⁸ is used to highlight atrial activations, thus making their detection easier. Although this approach has proven to be useful to facilitate activation detection⁸ as well as to quantify the dominant frequency (DF) of AF from the EGM,⁹ the resulting waveform morphology as well as the DF estimation can sometimes be significantly altered, as will be quantitatively demonstrated in the present work. Therefore, regular EGM preprocessing should be used carefully, or even avoided, over applications relying on EGM analysis that go beyond considering exclusively activation times.

On the other hand, although filtering can alter EGM amplitude, timing and morphology,⁵³ its effect on parameters widely used to characterize both in time and frequency the EGM has not been quantified yet. The goal of the present work is therefore to analyze the ability of regular preprocessing approaches to preserve waveform integrity and reduce noise both from unipolar and bipolar EGM recordings. In addition, alternative and efficient denoising methods successfully applied to the ECG will be explored and proposed.²⁸ The manuscript will prove that methods based on the Wavelet transform (WT) and the empirical mode decomposition (EMD) are able to provide cleaner and less morphologically altered EGM recordings, thus resulting in an optimal starting point for the proper interpretation of invasive AF recordings and a more truthful and accurate quantification of atrial activity dynamics.

The remainder manuscript is organized as follows. "Methods" section describes the analyzed databases containing synthesized and real EGMs as well as the proposed denoising algorithms. In this section the parameters used to quantify noise reduction and EGM morphology preservation reached by each algorithm are also presented briefly. "Results" section summarizes the obtained outcomes, which are then commented in "Discussion" section. Finally, "Conclusions" section presents the concluding remarks of this study.

METHODS

Study Population

The proposed denoising algorithms have been first validated using a database of synthesized unipolar and bipolar EGM recordings, since these signals allow to quantify accurately the achieved noise reduction as well as waveform integrity preservation. To mimic EGMs as realistic as possible, an approach similar to the one presented by Oesterlin *et al.*⁴² was used. Thus, atrial activations from a dataset of 40 real EGMs (20 unipolar and 20 bipolar) were manually annotated by two experts. These signals were acquired with a sampling frequency of 1000 Hz after a band-pass filtering between 0.5 and 500 Hz and a band-stop filtering around 50 Hz. Moreover, to avoid far-field ventricular contamination, they were also recorded under adenosine administration.⁵ This drug caused a transient atrioventricular block with a duration between 5.5 and 8.6 s and, therefore, only atrial activations were recorded during this interval. A window of 90 ms in length was then centered on each atrial activation, such that all were aligned in time. Next, sets of 10 single activations were averaged to generate noise-free templates. Every activation entered the template just in case its cross-correlation with the other template members was higher than 95%. A total of 18 and 26 templates for unipolar and bipolar recordings were respectively collected and normalized in amplitude. To synthesize an artificial EGM, a template was randomly selected and the probability of including others in the EGM was weighted with a gaussian distribution adapted to their cross-correlation. The DF for each

recording was randomly chosen between 3 and 12 Hz and the distance between successive atrial activations was generated by a normal distribution centered on that frequency with a standard deviation of 25 ms. Finally, the amplitude of the atrial activations was also modulated according to real signals. For that purpose, the upper and lower envelopes of real EGMs were extracted by cubic splines interpolation. Sets of 100 unipolar and 100 bipolar realistic, completely clean and 7 second-length EGMs were generated. This clean signal will be referred to as $x(n)$ from now on.

To assess the performance of the proposed denoising algorithms, standard EGM noise had to be added, thus obtaining noisy recordings referred to as $\tilde{x}(n)$. The noise was generated following the approach described in Ref. 14. Briefly, it was modeled as an autoregressive (AR) system, whose coefficients were derived by curve fitting from the gaps between atrial activations of real EGMs. The optimal order for the AR model was estimated by the Akaike information criterion, ranging from 10 to 35 for each analyzed EGM interval.⁷ Thus, choosing randomly an order within this range and the mean coefficients for all the real signals, different noise sets were synthesized and normalized in amplitude to generate EGMs with values of SNR of 30, 25, 20, 15, 10 and 5 dB. Figure 1 shows an example of unipolar and bipolar recordings synthesized with different levels of noise.

For the evaluation of the proposed algorithms over real scenarios, the aforementioned set of 40 real EGMs was doubled, so that a total of 80 real EGMs (40 unipolar and 40 bipolar) were analyzed. The study protocol was approved by the Institution's Research and Ethics Committee and all the enrolled patients

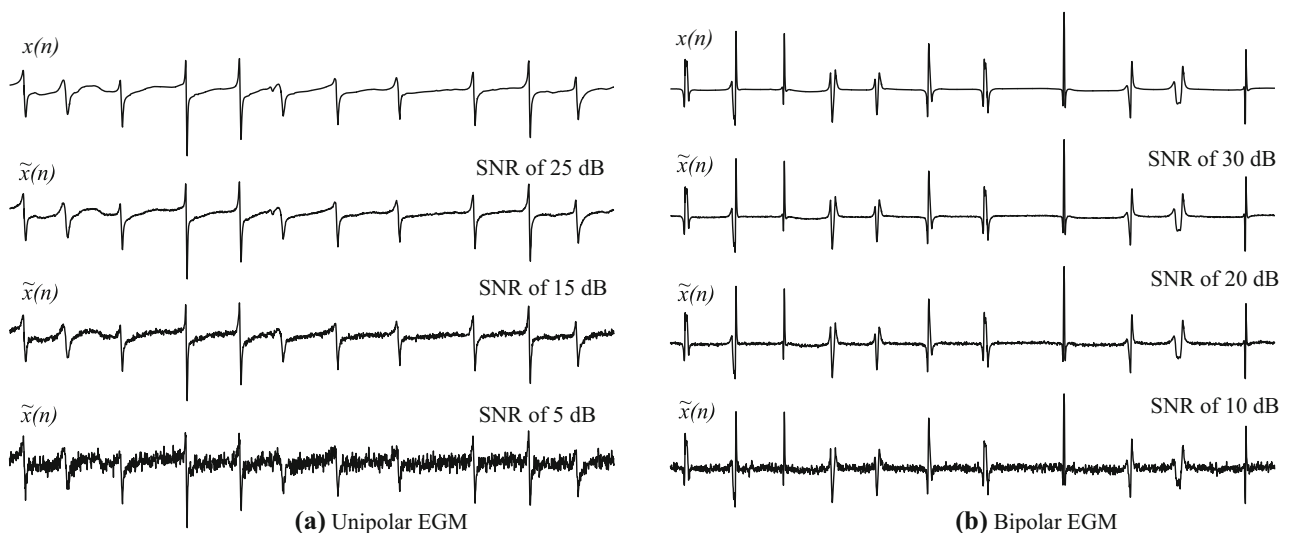


FIGURE 1. Example of two second-length synthesized recordings of unipolar (a) and bipolar (b) EGMs in AF with increasing levels of noise. The first row corresponds to clean EGMs, $x(n)$. The amount of added noise is different for unipolar than for bipolar synthesized recordings just to provide a better graphical idea on the noisy recordings, $\tilde{x}(n)$.

provided informed written consent. All signals were acquired from 50 different patients undergoing catheter ablation of AF. The expansion with the second group of real recordings was included with the aim to minimize any bias that could arise due to the set of synthesized recordings.

Studied Denoising Methods for EGM Acquisition

Next subsections describe the filtering approach regularly applied to EGM recordings. Next, alternative efficient methods applied to ECG noise reduction will be described and adapted to the case of intracardiac unipolar and bipolar EGM recordings.

Regular EGM Denoising

Some atrial structures, such as the pulmonary veins, can produce very rapid deflections with a substantial high-frequency content.⁵⁵ Thus, as an optimal trade-off between noise reduction and clinical information preservation, both unipolar and bipolar EGMs are regularly low-pass filtered with a cut-off frequency around 300 Hz.^{38,53} Contrarily, both kinds of recordings are often high-pass filtered with different cut-off frequencies. Indeed, this lower corner frequency is rarely higher than 3 Hz for unipolar EGMs.²⁶ In this way baseline wander is removed and some clinical information is preserved. Moreover, filtering at higher corner frequencies has proven to alter recording morphology, thus obscuring the proper detection of the wavefront propagation direction, which is the typical target in unipolar EGMs.⁵³ Surprisingly, although bipolar EGMs are more robust to noise than unipolar ones, since the two electrodes capture a similar far-field contamination which can be easily reduced by subtraction, a more aggressive high-pass filtering with a higher cut-off frequency of about 30 Hz has been regularly applied to these recordings.²⁶ In fact, the main goal of this preprocessing step is to reduce far-field ventricular contamination. However, the main atrial component, normally between 3 and 12 Hz in AF,¹³ is also strongly reduced. Obviously, this operation distorts substantially the EGM morphology and reduce its amplitude, thus turning the recording more complex and fractionated due to the severe reduction of its main atrial component.²⁶ Nonetheless, a variety of clinical studies have reported that some useful information still remains in the signal.⁵³ With the aim to reproduce the same steps of regular filtering, the synthesized recordings were pre-processed by second-order digital Butterworth filters following a forward/backward filtering strategy, which avoided the introduction of any phase delay.³³ The bandwidth of the applied filters was 3–300 and 30–300 Hz for unipolar and bipolar EGM recordings, respectively.

Wavelet Transform Denoising

Given its interesting ability to deal with non-stationary signals containing sharp spikes and discontinuous intervals, the WT has been widely used for ECG denoising.⁵¹ This transformation allows to decompose a signal at different time and frequency scales. Indeed, it can be defined for the continuous signal $x(t)$ as

$$C_a(b) = \int_{-\infty}^{\infty} x(t)\psi_{a,b}^*(t)dt, \quad (1)$$

where the asterisk stands for the complex conjugate operation and $\psi_{a,b}(t)$ represents scaled and translated versions of the basis function $\psi(t)$, named *mother wavelet*, such that

$$\psi_{a,b}(t) = |a|^{-\frac{1}{2}}\psi\left(\frac{t-b}{a}\right). \quad (2)$$

The factors of scale a and translation b have to meet two conditions, i.e., $a, b \in \mathbb{R}$ and $a \neq 0$. Obviously, the resulting wavelet coefficients $C_a(b)$ depend on these factors, such that if they are discretized for only taking integer values power of two (i.e., $a = 2^j$ and $b = k \cdot 2^j$), non-redundant information is obtained.³⁴ This discrete WT (DWT) has been widely used in biomedical applications,¹ since it can be easily implemented by a bank of low-pass and high-pass finite impulse response filters followed by decimation stages, such as Fig. 2 displays. The signals obtained from the high-pass and low-pass filtering processes consist of the detail $DC_j(k)$ and approximation wavelet coefficients $AC_j(k)$, respectively.

A generalization of this transformation able to offer additional information is the Wavelet packet transform (WPT).³⁴ In contrast to the DWT, where only approximation coefficients are low- and high-pass filtered, both detail and approximation coefficients are split at each level into finer components. In this case optimal decomposition can be obtained by minimizing the entropy during the process.⁵⁴ Thus, a vector of wavelet coefficients is only split when the entropy is reduced. Although several approaches have been proposed to compute entropy from wavelet coefficients, the common Shannon Entropy (ShEn) has been used in this work.³⁴ Both DWT and WPT have been applied to the recordings, so that once the noisy EGM $\tilde{x}(n)$ was decomposed into a specific number of scales, the wavelet coefficients were thresholded and used to reconstruct back a denoised signal $\hat{x}(n)$.⁵¹

Two thresholding rules, i.e., hard and soft, have been widely used for ECG denoising.³⁰ In hard thresholding the wavelet coefficients below a threshold λ are set to zero, whereas in soft thresholding coefficients lower than λ are set to zero and the remaining ones are reduced by that value.⁵⁴ Obviously, the

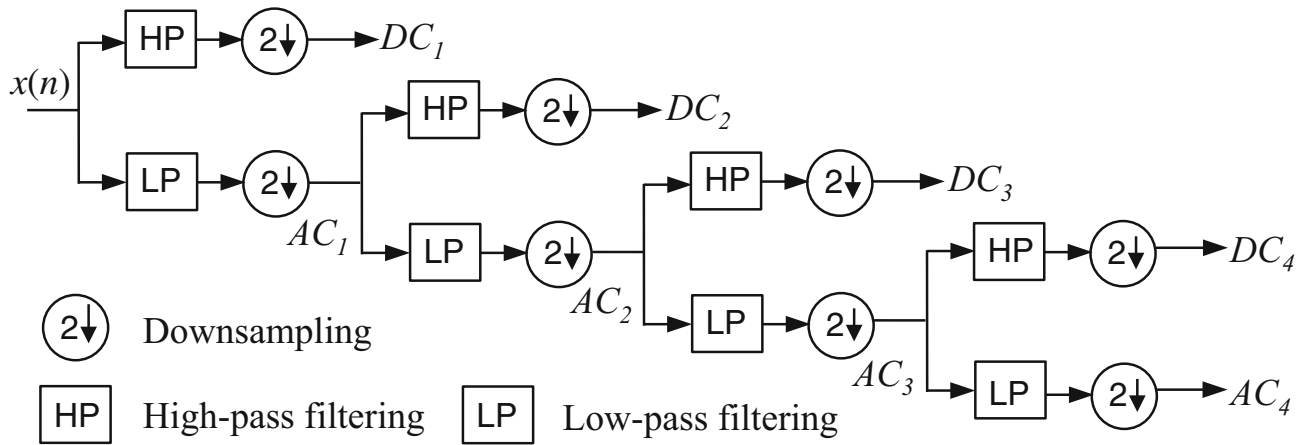


FIGURE 2. Detail of the filter bank structure for DWT computation.

thresholding rule together with the value of λ determine the resulting signal. Hence, all possible combinations between hard and soft thresholding rules and the most typical approaches to compute λ have been analyzed both for DWT and WPT.

To this last respect, considering jointly all the wavelet coefficients from a decomposition, thus producing a vector of S samples in length, two different values of λ have been first defined following¹⁶

$$\lambda_{\text{FIX}} = \sqrt{2 \cdot \ln(S)}, \quad (3)$$

which stands for a fixed thresholding rule for all the wavelet scales, and

$$\lambda_{\text{MMX}} = 0.3936 + 0.1829 \cdot \log(S), \quad (4)$$

which performs a minimax estimation of the thresholding rule for every decomposition level. In addition, an adaptive threshold for each vector of wavelet coefficients has also been computed from the Stein's unbiased risk estimate (SURE), i.e.,

$$\lambda_{\text{SURE}} = \sqrt{2 \ln(S_C \cdot \log_2(S_C))}, \quad (5)$$

where S_C is the length of the analyzed vector.¹⁷ Finally, a variant of this approach (named heuristic SURE, λ_{HSURE}) where λ_{SURE} was replaced by λ_{FIX} in very noisy conditions, has also been considered following the recommendations in Ref. 17. For a more effective denoising, these thresholds were rescaled by the standard deviation of the noise estimated from the highest frequency vector of wavelet coefficients.¹⁶ The standard deviation was computed as

$$\hat{\sigma} = \text{median}_{k=1, \dots, S_{C_1}} \{|C_1(k)|\} / 0.6745. \quad (6)$$

Finally, it has to be noted that no systematic approach exists for optimal selection of the mother wavelet, even though the use of different functions to analyze the same signal can sometimes produce no-

tably different results.⁴⁵ In denoising applications, the mother wavelet is normally determined by its similarity with the fundamental signal pattern under analysis. In this way the highest wavelet coefficients are obtained in the decomposition, thus turning thresholding of contaminant signals easier.⁵¹ In the present study, all the functions from the most common orthogonal and biorthogonal wavelet families, including Daubechies, Biorthogonal, Coiflets, Symlets, Reverse Biorthogonal and Discrete Approximation of Meyer, were tested. A total of 54 functions were then studied. Note that, only when orthogonal functions are used, the information stored in each vector of wavelet coefficients is not repeated elsewhere and the original signal can be accurately reconstructed. On the other hand, the number of decomposition levels is also a key parameter to achieve satisfactory results. The maximum level depends on the length of both the signal and the decomposition filter.⁴⁵ In this case, that value was 8 and, hence, decomposition levels between 3 and 8 were analyzed.

Empirical Mode Decomposition Denoising

In contrast to WT, EMD does not require any *a priori* known basis to decompose a signal into a set of oscillatory components ranging from high to low frequencies, which are named intrinsic mode functions (IMFs).²⁵ Hence, this transform also behaves as a filter bank, but without a predefined cut-off frequency.²⁰ This property makes EMD especially useful for the processing of nonlinear and non-stationary signals. Indeed, it has been widely used for denoising of ECG as well as other physiological signals.^{6,32}

Every IMF must have the same number of extrema and zero-crossings or differ at most by one and, additionally, it must be symmetric with respect to local zero mean.²⁵ Thus, for a successful decomposition into IMFs, the signal must have at least two extrema, i.e.,

one maximum and one minimum. Given that any noisy recording $\tilde{x}(n)$ in the present study met this condition, the decomposition process started with the identification of all local maxima and minima in the signal. Next, these points were interpolated by a cubic spline curve to reconstruct the upper $e_u(n)$ and lower $e_l(n)$ envelopes, respectively. The mean envelope was obtained as a simple average, i.e.,

$$m(n) = \frac{e_u(n) + e_l(n)}{2}, \quad (7)$$

and, it was then subtracted from the contaminated signal to obtain

$$h_1(n) = \tilde{x}(n) - m(n). \quad (8)$$

The same process was iteratively repeated on the resulting signal $h_k(n)$ until the following condition was satisfied

$$\frac{|h_{k-1}(n) - h_k(n)|^2}{h_{k-1}(n)^2} \leq 0.3, \quad (9)$$

thus $h_k(n)$ being the first IMF, named $c_1(n)$. The residue $r_1(n) = \tilde{x}(n) - c_1(n)$ still contained useful information and, hence, the process was repeated on this signal to obtain $c_2(n)$. In the same way $c_3(n), \dots, c_{10}(n)$ were computed, such that the original signal could be reconstructed as

$$\tilde{x}(n) = \sum_{k=1}^{10} c_k(n) + r_{10}(n). \quad (10)$$

Bearing in mind that IMFs from the lower levels present higher frequency components and *vice versa*, previous works have proven that high-frequency noise can be successfully removed from some physiological signals by reconstructing the recording without the first functions.¹⁰ Consequently, the present work has analyzed EMD-based denoising performance by discarding up to 5 IMFs, such that

$$\hat{x}(n) = \sum_{k=K}^{10} c_k(n) + r_{10}(n), \quad \text{for } K = 2, \dots, 5. \quad (11)$$

Waveform Integrity and Noise Reduction Assessment

The ability to reduce noise and preserve waveform integrity of the proposed algorithms was validated in terms of time and frequency parameters widely accepted to characterize both unipolar and bipolar EGMs. Firstly, morphological alterations caused by the denoising methods were quantified by computing the cross-correlation and the root mean square error (RMSE) between every pair of denoised recording $\hat{x}(n)$

and its corresponding original signal $x(n)$. Since the common Pearson's correlation coefficient does not account for amplitude differences between signals, an adaptive signed correlation index (ASCI) was used for a more accurate morphological comparison.³¹ Considering N sample-length signals, the ASCI was defined as

$$\text{ASCI}(x(n), \hat{x}(n)) = \frac{1}{N} \sum_{k=1}^N x(k) \otimes \hat{x}(k), \quad (12)$$

where \otimes denotes the signed product of two dichotomized scalars as

$$x(n) \otimes \hat{x}(n) = \begin{cases} 1 & \text{if } |x(n) - \hat{x}(n)| \leq \beta, \\ -1 & \text{if } |x(n) - \hat{x}(n)| > \beta. \end{cases} \quad (13)$$

The threshold β was experimentally selected as 5% of the standard deviation of $x(n)$. Also, note that the RMSE was normalized to the root mean square of $x(n)$, i.e.,

$$\text{RMSE} = \sqrt{\frac{\sum_{k=1}^N (x(k) - \hat{x}(k))^2}{\sum_{k=1}^N x(k)^2}}. \quad (14)$$

A metric proposed to quantify the whole EGM morphology and, thus, to discern between fractionated and non-fractionated signals, is ShEn.³⁷ Hence, this parameter was also computed to assess morphological variations after denoising. In brief, the EGM was quantified using L uniform and equal-size amplitude levels. Then, the occurrence probability of the i th level (p_i) was estimated from its repetition rate and ShEn was computed as

$$\text{ShEn} = \frac{-1}{\log L} \sum_{k=1}^L p_k \cdot \log p_k. \quad (15)$$

Moreover, the morphological comparison between atrial activations has been widely used as a measure of AF organization, which has proven to be useful in a variety of clinical scenarios.⁴⁶ In contrast to the above defined indices ASCI, RMSE and ShEn, this morphological comparison only considers atrial activations themselves, thus discarding the remaining EGM content in between.¹⁹ Given that this methodology requires an accurate identification of every single activation, the algorithm introduced by Ng *et al.*⁴⁰ has been used in this study. More precisely, the EGM was first processed with the approach proposed by Botteron and Smith,⁸ i.e., the signal was band-pass filtered between 40 and 250 Hz, then rectified and, finally, low-pass filtered with a cut-off frequency of 20 Hz. Zero-phase third-order Butterworth filters were used. The peak with the highest amplitude in the resulting signal was marked as the first atrial activation. Next, peaks with decreasing amplitudes were identified considering a blanking period of 50 ms around each one. The

process finished when the mean distance between successive peaks was lower than 275 ms and, moreover, that distance was also lower than its median plus 5 ms or the detected peak magnitude was 20% less than the previous one.⁴⁰ Finally, activations within intervals 1.5 times greater than the median distance between successive peaks were also searched. The peaks detected from clean and denoised signals, $x(n)$ and $\hat{x}(n)$, were compared in terms of sensitivity (Se), positive predictivity (P^+) and location error (LE). Thus, Se was defined as the rate of atrial activations properly identified, whereas P^+ was the proportion of true activations from all detected. Lastly, the LE was defined as the time difference between activation locations in the clean signal with respect to the noisy one for every pair of $x(n)$ and $\hat{x}(n)$ considered.

Once the atrial activations were detected, morphological similarity among them was quantified through the algorithm presented by Faes *et al.*¹⁹ In brief, the barycenter for every atrial activation was identified using a moving average noncausal filter with 90 coefficients. Centered on this point, which divides the activation into two equal parts, a window of 90 ms was defined. To prevent morphological alterations from factors unrelated to the arrhythmia, each activation was normalized by the Euclidean norm of all atrial activations in the recording.¹⁹ Finally, a repetition rate of M activations was defined by computing the relative number of similar atrial activation pairs, so that

$$\rho(\xi) = \frac{2}{M \cdot (M - 1)} \sum_{i=1}^M \sum_{j=i+1}^M \Theta(\xi - d_{ij}), \quad (16)$$

where $\Theta(x)$ is the Heaviside function and d_{ij} is the distance between i th and j th activations, defined as the arc cosine of their scalar product.¹⁹ The threshold ξ was chosen as $\pi/3$ radians.¹⁹

The proposed denoising algorithms have been also validated from the spectral domain through the use of two indices. In fact, the goal of most frequency-domain techniques applied to EGMs in AF is to estimate the local atrial rate, i.e., the DF.³⁹ For that purpose, the preprocessing introduced by Botteron and Smith has been widely used and is applied by default in many recording systems.³⁹ Indeed, it has been proven that this approach removes detailed features of the atrial activations with the aim to emphasize their timing.⁹ In the present work, the resulting signal from every denoising method was spectrally characterized through the Welch Periodogram with a Hamming window of 4096 points in length, 50% overlapping and 10240-point FFT.¹⁸ These computational parameters provided a frequency resolution of 0.1 Hz. Next, the DF was computed as the peak with the highest spectral energy. Finally, to estimate spectral preservation, the regularity index (RI) was

computed due to its wide use as an estimator of AF organization in clinical studies.⁴⁸ The RI is defined as the power spectral density ratio of the 2 Hz band centered on the DF with respect to the physiological frequency range of AF, i.e., 3–20 Hz.

On the other hand, given that a completely clean signal is unavailable in real scenarios, the parameters introduced above cannot assess the performance of the denoising algorithms over real EGMs. For this case, the yielded noise reduction is assessed through the SNR estimated as the power ratio between the denoised signal and the corresponding extracted noise,⁵² i.e.,

$$\widehat{\text{SNR}} = 10 \cdot \log \left(\frac{\sum_{k=1}^N \hat{x}(k)^2}{\sum_{k=1}^N \hat{n}(k)^2} \right), \quad (17)$$

where the noise power is estimated as the power difference between the noisy and denoised recordings, so that

$$\sum_{k=1}^N \hat{n}(k)^2 = \sum_{k=1}^N (\bar{x}(k) - \hat{x}(k))^2. \quad (18)$$

A perfect denoising stage will extract all the noise and only the noise. Thus, yielding the same result in estimated $\widehat{\text{SNR}}$ than the real SNR of the recording. On the contrary, a poor denoising stage will not remove all the noise, or even potentially will consider part of the signal as noise. Hence, $\widehat{\text{SNR}}$ will be far away from the real SNR, indicating that noise still remains or that part of the signal has been considered as noise and removed. As a consequence, the ratio between $\widehat{\text{SNR}}$ and SNR will not be one to one. For synthesized EGM recordings and with the aim to validate the index, $\widehat{\text{SNR}}$ has been directly compared to the generated SNR. For real EGM recordings and each denoising methodology, the estimated $\widehat{\text{SNR}}$ has been compared with the optimally estimated $\widehat{\text{SNR}}_O$, that was provided by the denoising approach with best results in the synthesized signals.

Finally, note that all the described algorithms have been developed under Matlab 8.6, which is a popular mathematical programming platform from The MathWorks, Inc. Moreover, they have been run on a desktop computer with 3.2 GHz Intel Core i5 processor under Mac OS X 10.11.6, thus providing the results that will be presented in the forthcoming section.

RESULTS

Synthesized EGM Recordings

The effect of noise on the synthesized recordings is quantified in Table 1. Some of the parameters are preceded by a Δ thus representing normalized relative

TABLE 1. Morphological alteration results caused by noise addition on the synthesized recordings as a function of the signal-to-noise ratio (SNR).

EGMs	SNR (dB)	ASCI (%)	RMSE (%)	ΔShEn (%)	$\Delta\rho$ (%)	Se (%)	P^+ (%)	LE (ms)	ΔDF (%)	ΔRI (%)
Unipolar	30	99.9	0.1	0.2	1.1	99.2	99.7	0.053	0.8	4.1
	25	98.2	0.3	0.5	3.0	97.9	98.9	0.085	1.0	7.6
	20	84.7	0.9	1.0	7.9	97.9	94.6	0.155	2.4	13.5
	15	58.9	3.1	2.4	12.2	98.8	91.1	0.288	10.0	23.7
	10	35.7	9.9	5.1	19.9	94.2	85.2	0.505	29.2	39.8
	5	20.7	31.6	9.5	47.0	93.0	63.5	0.889	50.2	60.9
Bipolar	30	99.9	0.1	0.7	1.8	99.9	99.6	0.052	2.9	4.0
	25	95.6	0.3	1.7	6.1	99.3	97.3	0.099	2.8	6.7
	20	78.4	1.0	3.8	11.6	98.9	92.7	0.176	4.7	11.7
	15	53.8	3.1	7.5	17.0	98.6	89.1	0.298	7.6	19.4
	10	32.9	9.9	13.0	25.7	96.9	88.1	0.538	10.0	32.4
	5	19.0	31.6	21.1	56.3	95.1	68.1	0.899	13.9	53.0

Displayed results stand for adaptive signed correlation index (ASCI), root mean square error (RMSE), Shannon entropy variation (ΔShEn), variation of similarity between atrial activations ($\Delta\rho$), sensitivity, positive predictivity and location error of atrial activation detection (Se, P^+ , LE), dominant frequency variation (ΔDF) and regularity index variation (ΔRI). In the case of ΔShEn , $\Delta\rho$, ΔDF and ΔRI the variation has been computed as the difference between clean, $x(n)$, and noisy signals, $\tilde{x}(n)$, normalized by $x(n)$ and expressed in percentage.

variations between clean and noisy recordings. As can be observed, the defined indices are able to reflect accurately how the presence of increasing levels of noise degrade the EGM waveform morphology and alter its time and frequency features. Although this finding applies both to unipolar and bipolar EGM signals, a slightly different behavior between both kinds of recordings was observed in some cases, as for ΔShEn and ΔDF . Thus, the bipolar signals were more sensitive to noise in terms of ΔShEn , while an opposite trend was noticed for ΔDF . Another interesting finding is that P^+ decreased notably as the noise increased, thus highlighting a substantial rise in the number of falsely detected atrial activations under noisy conditions.

Regarding how atrial waveform integrity is preserved by the analyzed denoising methods, the main outcomes are summarized in Fig. 3 for synthesized unipolar EGMs. This figure only displays the best results for DWT-, WPT- and EMD-based denoising algorithms. Additional results obtained from a wider variety of tested parameters for each denoising strategy can be found in the online section of Supplementary Materials. No significant differences were noticed both for DWT and WPT from the analyzed wavelet functions, wavelet levels of decomposition, thresholds and thresholding rules. Nonetheless, for DWT the highest degree of waveform morphology preservation and noise reduction was achieved with the second-order Coiflet function with 8 decomposition levels and soft thresholding using λ_{SURE} . With these parameters, WPT also provided good results, however its highest performance was obtained with the second-order Daubechies function selecting 5 decomposition levels and soft

thresholding using λ_{HSURE} . Finally, the EMD-based technique provided the highest waveform integrity by discarding the first IMFs, i.e., for $K = 2$.

Coherently, most of the tested methods provided more altered features of signal morphology and frequency content as the SNR decreased. However, the two WT-based algorithms provided the cleanest and most unaltered unipolar recordings. Their performance was superior to that of regular filtering in any analyzed case and they provided especially good results for moderate or high levels of noise. Observe in Fig. 3 how regular filtering alters waveform morphology and how EMD provided poorer results than WT-based methods. Thus, even for the most favorable case with a clean recording of 30 dB in SNR, the gap in waveform integrity preservation between regular filtering and WT-based methods was significantly large. Metrics such as ASCII or RMSE provided improvements in waveform preservation of about 20% (ASCII of 79.2% vs. 99.9%). Furthermore, in noisy cases, such as SNR of 5 dB, the waveform alteration introduced by regular filtering was extremely high compared to WT-based methods (ASCII of 26.8 vs. 60.4%). Other interesting observation refers to ΔDF because the detected dominant frequency variation has been always notably higher for regular filtering, thus involving deviations of up to 37.2%. Taking into consideration the relevance that tiny differences in dominant atrial frequency maps have reached in recent works as a tool for guiding catheter ablation,⁴ this finding is of great interest.

Regarding synthesized bipolar recordings, Fig. 4 summarizes the obtained results. As before, only the best denoising results are included, so that the remaining additional outcomes can be found in the online section of Supplementary Materials. As in the

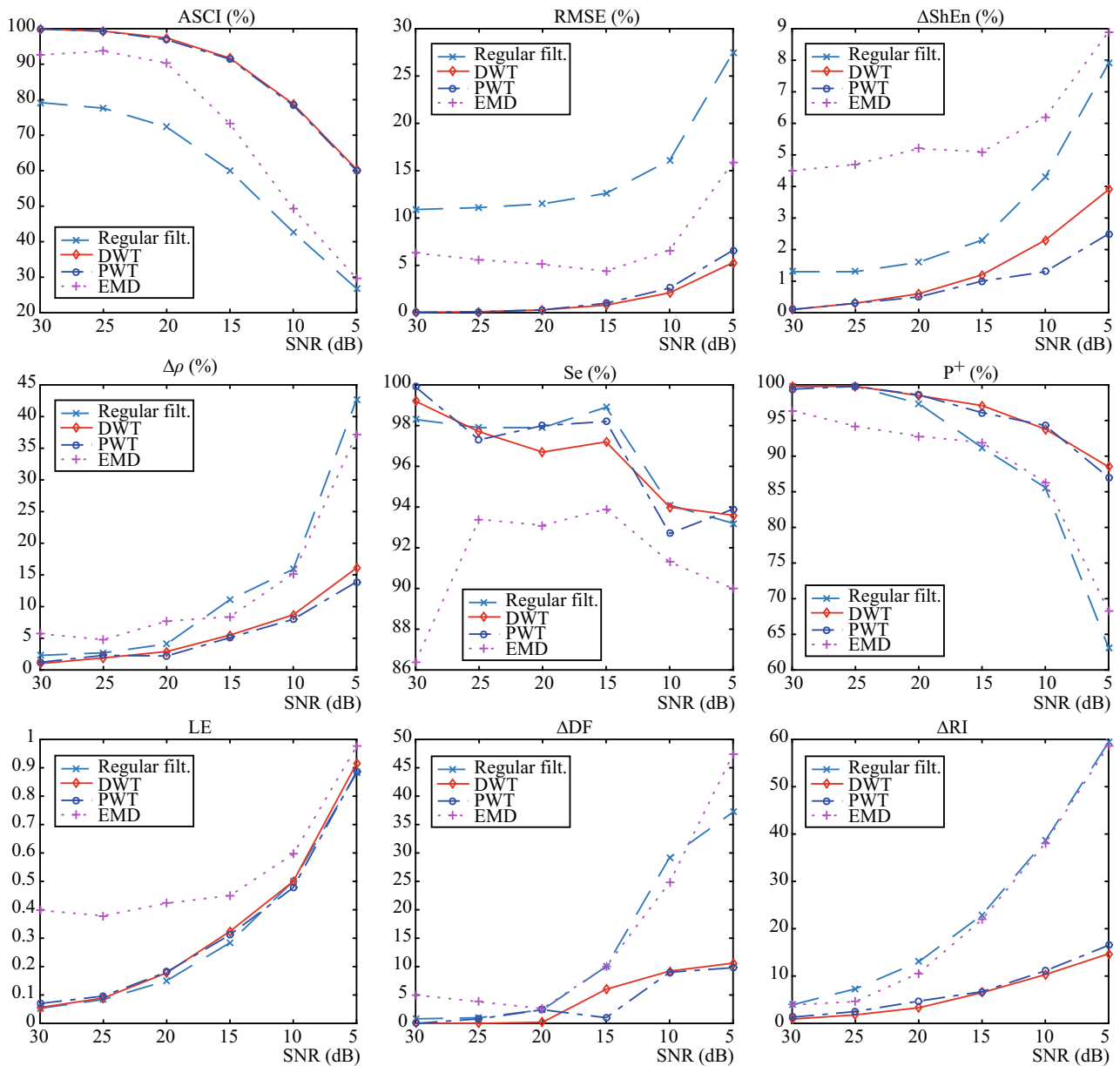


FIGURE 3. Waveform integrity preservation and time and frequency indices provided by the analyzed algorithms as a function of noise for synthesized unipolar EGMs. Note that second-order Coiflet and second-order Daubechies wavelet functions were used for DWT and PWT, respectively.

unipolar case, most of the methods provided poorer results as noise increased. The exception to this rule was regular filtering, in which a significant high degree of waveform distortion was introduced for any SNR. More concretely, in the most favorable case with SNR of 30 dB, regular filtering distorted notably the atrial waveform in comparison to WT-based methods (ASCI of 39.6 vs. 99.8%). In fact, the presence of such a low level of noise did not distort the atrial waveform, but regular filtering provoked considerable distortion levels by itself. Bearing in mind that such a kind of filtering is the most extended procedure in routine

analysis of bipolar EGMs, this result is also specially significant. Furthermore, it has to be highlighted the poor outcomes provided by EMD which, in some cases, were below regular filtering as Se, LE or ΔDF .

Finally, the relation between average values of estimated \widehat{SNR} and generated SNR for synthesized recordings is graphically sketched in Fig. 5. As has been detailed back in “Waveform Integrity and Noise Reduction Assessment” section, the \widehat{SNR} has been defined to estimate noise reduction performance on real EGMs. However, its application to synthesized

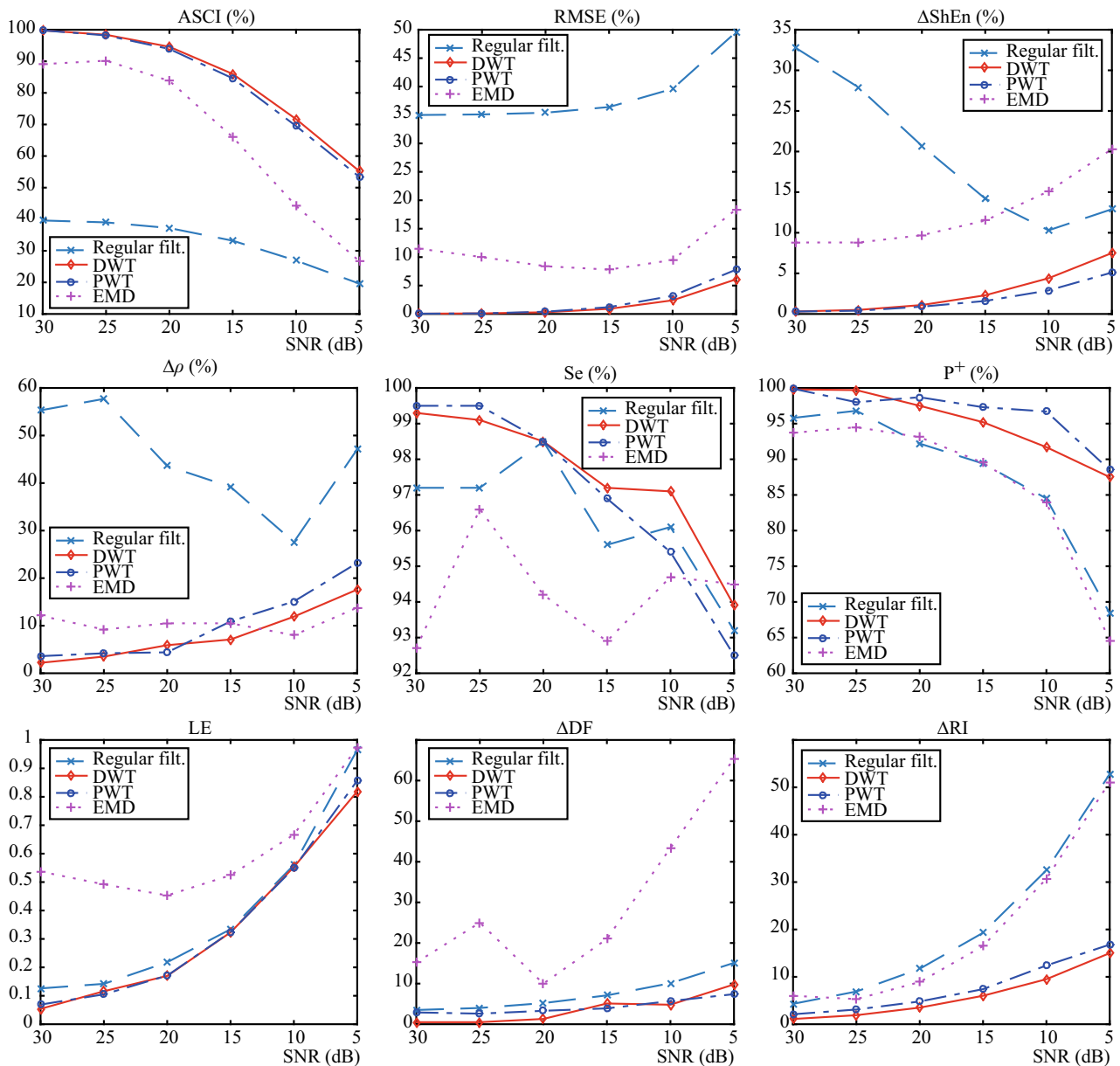


FIGURE 4. Waveform integrity preservation and time and frequency indices provided by the analyzed algorithms as a function of noise for synthesized bipolar EGMs. Note that second-order Coiflet and second-order Daubechies wavelet functions were used for DWT and PWT, respectively.

EGMs is also of interest in order to verify its validity and robustness. Two main considerations can be done in view of the results for synthesized EGMs. Firstly, WT-based methods present a clearly linear and progressive relation between $\widehat{\text{SNR}}$ and SNR, thus indicating that they are quite close to an ideal denoising approach. In fact, these strategies are able to remove most part of the noise in the recording and only the noise. Secondly, EMD and especially regular filtering do not present a one-to-one ratio between estimated and generated SNRs. Therefore, these methods are unable to remove a significant part of the noise in the

signal or, even worse, they also remove part of the signal which is mistakenly considered as noise.

Real EGM Recordings

The only parameter that can be used to assess noise reduction performance as well as waveform preservation when dealing with real recordings is the estimated $\widehat{\text{SNR}}$. To this respect, Fig. 6 shows the ratio between $\widehat{\text{SNR}}$ and optimally estimated $\widehat{\text{SNR}}_O$, as described back in “[Waveform Integrity and Noise Reduction Assessment](#)” section. This last index was computed

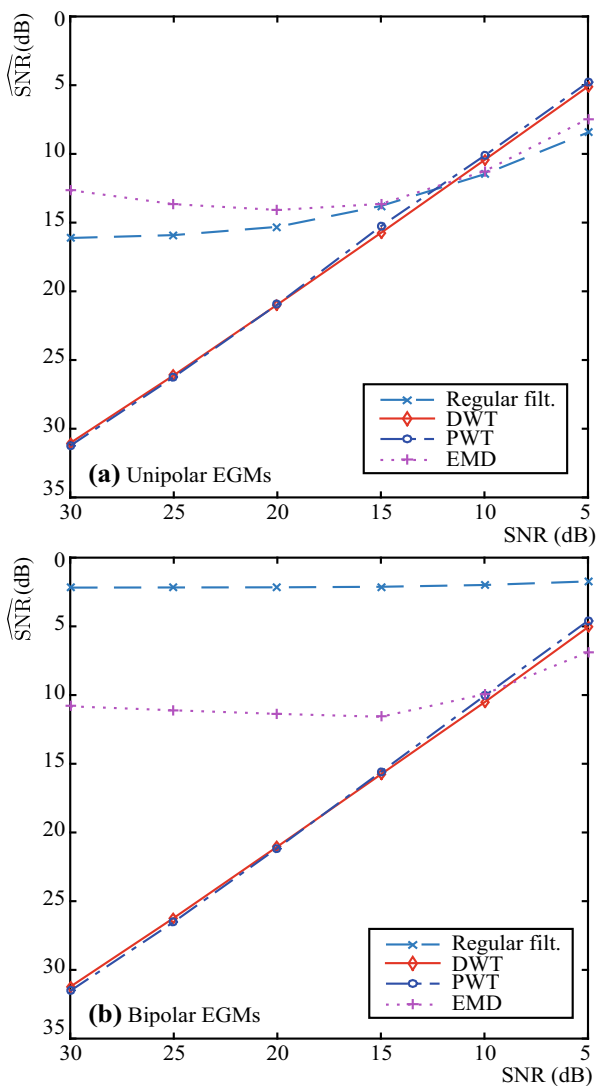


FIGURE 5. Relation between estimated $\widehat{\text{SNR}}$ and generated SNR achieved by every denoising algorithm in the case of (a) synthesized unipolar EGMs and (b) synthesized bipolar EGMs. Note that second-order Coiflet and second-order Daubechies wavelet functions were used for DWT and PWT, respectively.

making use of the DWT-based denoising strategy to obtain results for regular filtering, PWT-based and EMD-based methods because DWT yielded the best noise reduction and waveform preservation results with synthesized recordings. In the case of DWT-based denoising, the $\widehat{\text{SNR}}_O$ was provided by the PWT-based approach, which also provided excellent results. In view of the results for real recordings in the figure, the WT-based methods offered a denoising and waveform preservation behavior with outstanding performance. Thus, the estimated $\widehat{\text{SNR}}$ followed a clear line very close to the one-to-one ratio with $\widehat{\text{SNR}}_O$. This is indicative of the great ability that these methods pro-

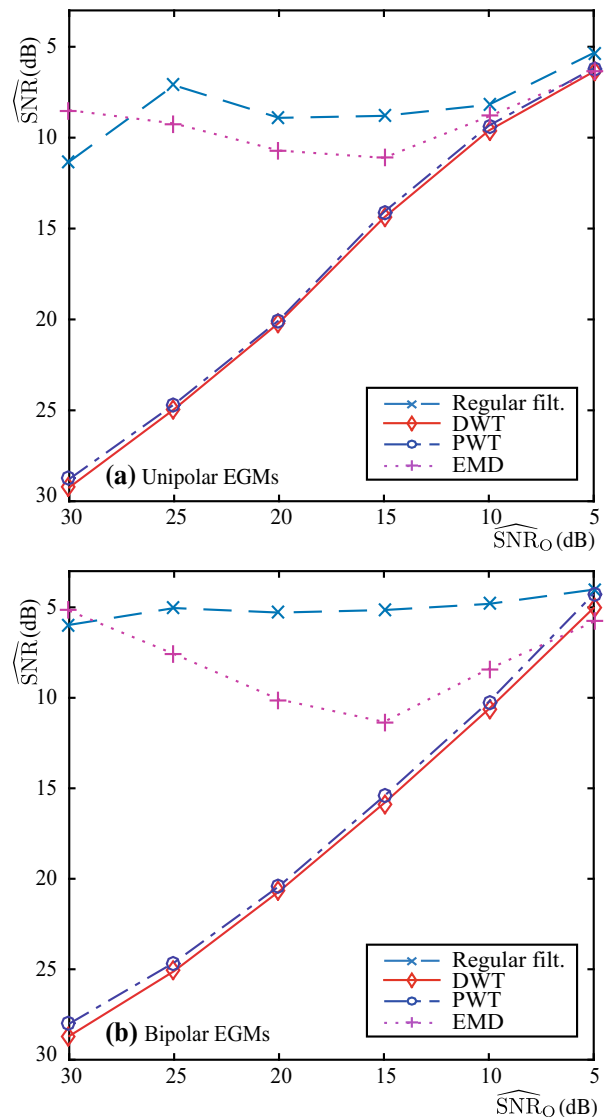


FIGURE 6. Relation between estimated $\widehat{\text{SNR}}$ and optimally estimated $\widehat{\text{SNR}}_O$ achieved by every denoising algorithm in the case of (a) real unipolar EGMs and (b) real bipolar EGMs. Note that second-order Coiflet and second-order Daubechies wavelet functions were used for DWT and PWT, respectively.

vide for removing most part of the noise and only the noise, both in unipolar and bipolar recordings. On the contrary, EMD and especially regular filtering, presented a significantly limited ability of noise reduction and waveform preservation even in the most favorable cases of very low noise with SNR of 30 dB.

Finally, with the aim to provide a wide overview on the performance of the analyzed denoising strategies over real EGMs, Figs. 7 and 8 show a set of examples for unipolar and bipolar real EGMs, respectively, with different morphologies and levels of noise, together with the corresponding result provided by each methodology. As can be observed, even for reduced

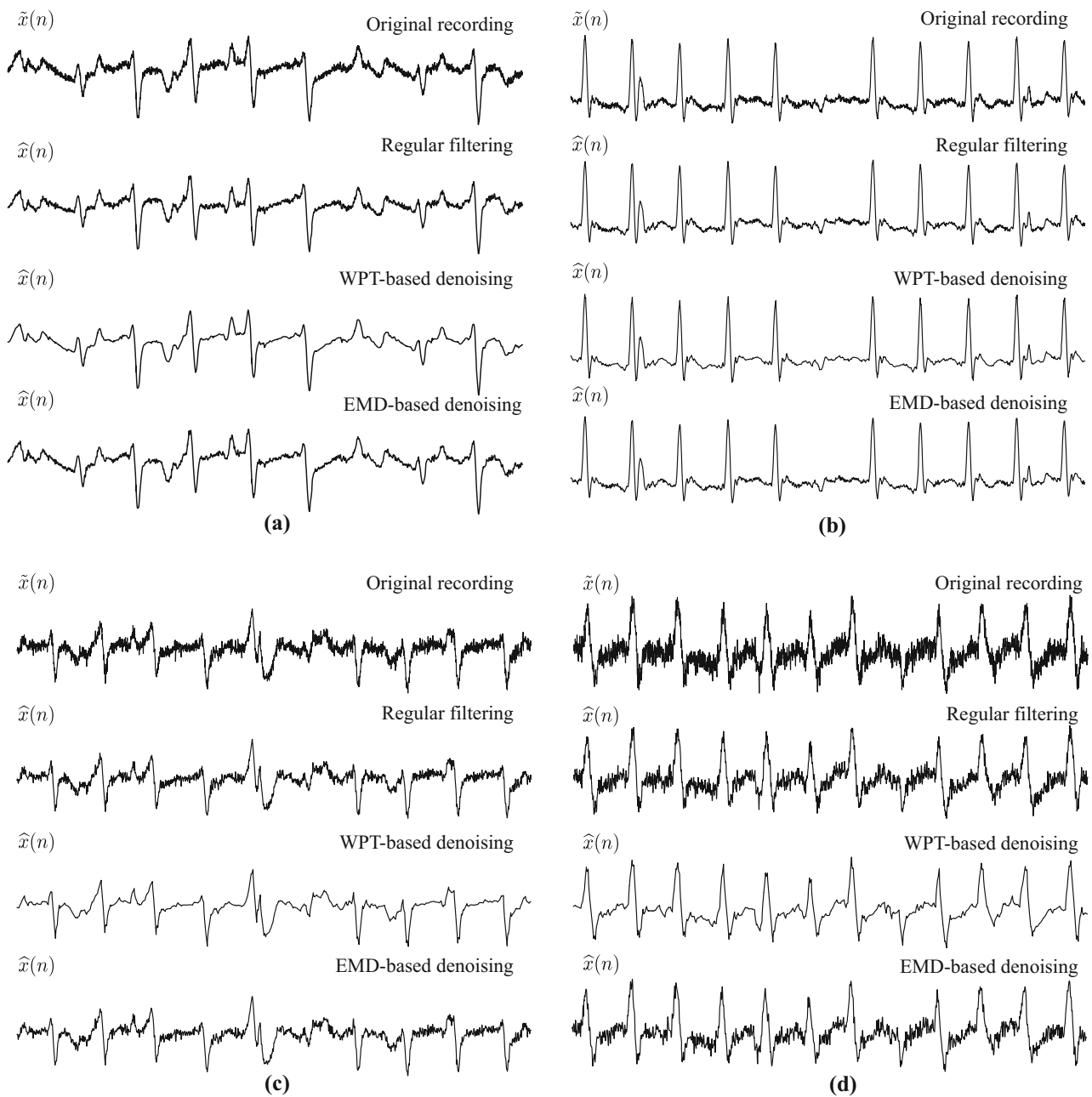


FIGURE 7. Example of waveform integrity preservation and denoising performance of the analyzed methods for real unipolar EGMs under different noisy conditions. The noisy recording $\tilde{x}(n)$ is filtered out by the different methodologies to provide the denoised resulting EGM $\hat{x}(n)$. The estimated SNR in every case is (a) 20 dB, (b) 17 dB, (c) 13 dB and (d) 10 dB, respectively.

noise (Figs. 7a, 7b and 8a, 8b), regular filtering performs extremely poor in EGM denoising compared to WT-based methods, whereas EMD performs quite better than regular filtering but poorer than DWT or WPT. Furthermore, waveform integrity is completely reduced and altered in bipolar EGMs processed by regular filtering. On the other hand, when the EGM is relatively noisy (Figs. 7c, 7d and 8c, 8d) WT-based methods still behave with outstanding performance, while EMD is unable to remove noise with similar

efficiency but does not seem to provoke significant waveform distortion. In contrast, regular filtering performs extremely bad both in EGM denoising and waveform integrity preservation, especially in the bipolar case. Observe how resulting amplitudes are notably reduced, even provoking the masking of some atrial activations inside the noise. Obviously, amplitude reduction as well as activation timing lost are the potential source of significant variations in voltage cartography, activation maps, rotor maps or any other

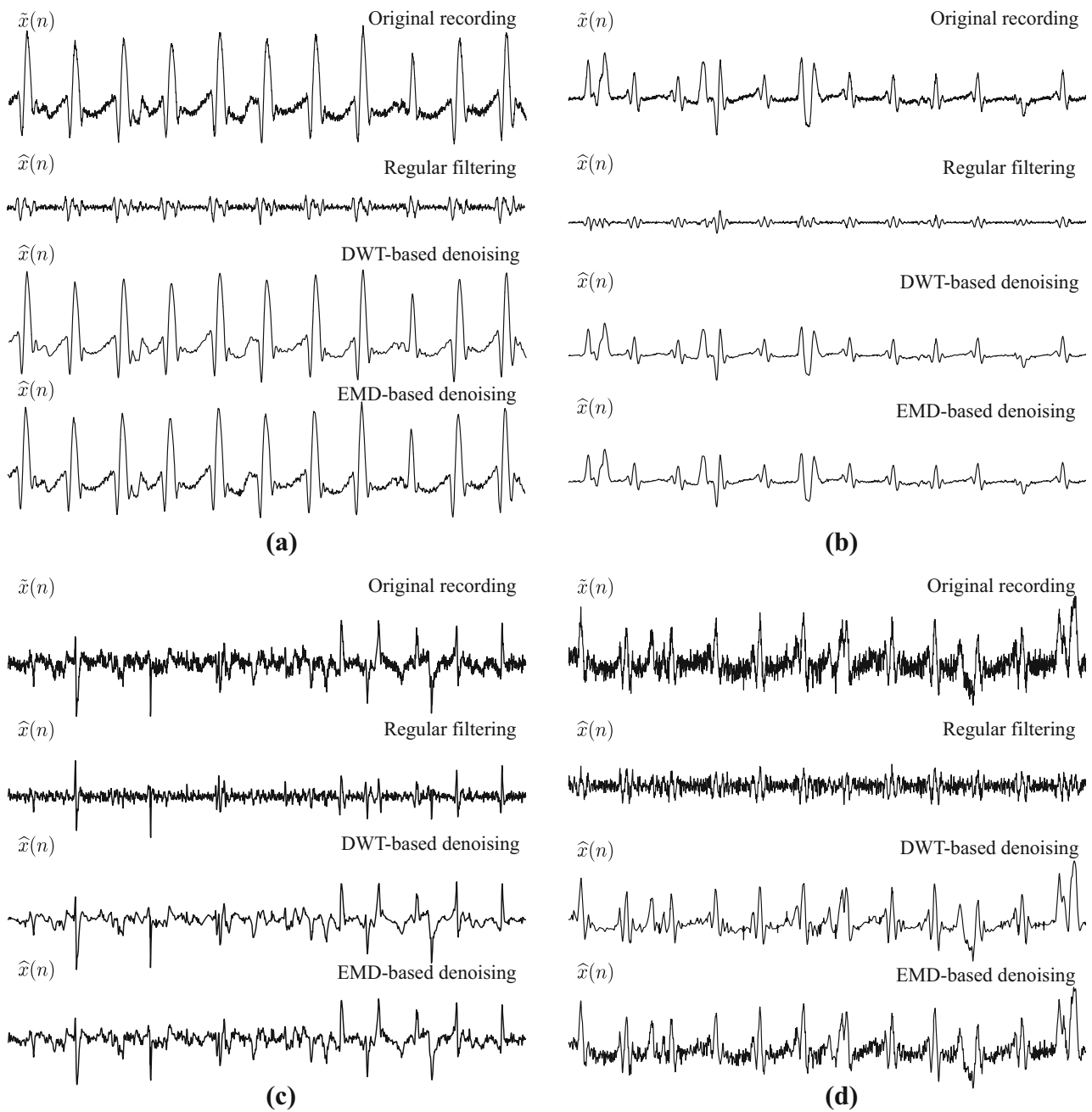


FIGURE 8. Example of waveform integrity preservation and denoising performance of the analyzed methods for real bipolar EGMs under different noisy conditions. The noisy recording $\tilde{x}(n)$ is filtered out by the different methodologies to provide the denoised resulting EGM $\hat{x}(n)$. The estimated SNR in every case is (a) 20 dB, (b) 18 dB, (c) 12 dB and (d) 9 dB, respectively.

operation performed with bipolar EGMs in cardiac mapping systems.

DISCUSSION

The surface ECG, although highly sensitive to noise, still is the most widely used recording for cardiac diagnosis.³³ Indeed, noise reduction strategies applied to the ECG have been widely addressed in the last

years to improve its characterization and interpretation.³³ As a result, a broad variety of denoising methods are available in the literature, including filter banks, adaptive filtering, independent component analysis, neural networks, WT and EMD.²⁸ Contrarily, noise reduction applied to EGMs has received poor attention. Although intracardiac recordings are often less disturbed by noise than the surface ECG, nuisance interferences are still present during its acquisition⁵⁵

and, therefore, this issue has to be properly addressed. Thus, the exploration of new algorithms to reduce noise in the EGM but, at the same time, preserving waveform integrity still is an unsolved challenge. In fact, most of the EGM recording systems regularly filter quite aggressively the acquired signal,²⁶ even though this preprocessing has proven to alter its morphology. Within this context, the present work has introduced the first systematic and thorough comparison between regular filtering and more refined algorithms, successfully used in ECG denoising, applied to the EGM. The coherence between the results obtained both from synthesized and real EGMs allows us to present some remarkable observations as well as useful recommendations about EGM preprocessing, which will be next picked out.

Comparison Among EGM Denoising Algorithms

To begin with, regular filtering has provided very poor performance in waveform integrity preservation as well as in noise reduction compared to WT-based methodologies. Thus, under low noise conditions, variations of about 20% in waveform preservation were noticed for unipolar EGM recordings between regular filtering and WT-based denoising (see Fig. 3). Furthermore, the bipolar case was even worse, and variations of about 60% in ASCI or RMSE were observed (see Fig. 4). In fact, parameters like ΔShEn and $\Delta\rho$ behaved very poorly with regular filtering regardless of the SNR. For noisy cases the situation remained the same for some indices and even worse for many others. Thus, for unipolar EGM recordings parameters like $\Delta\rho$, P^+ , ΔDF and ΔRI increased the gap between regular filtering and WT-based methods, whereas in the case of bipolar recordings indices like P^+ or ΔRI also performed poorer than for low noise conditions. The significant and high-amplitude components between 1 and 30 Hz eliminated by the aggressive regular filtering clearly justify these outcomes. Moreover, this fact also explains the notably low estimated $\widehat{\text{SNR}}$ by this filtering than the remaining denoising algorithms, as Figs. 5 and 6 show for unipolar and bipolar EGM recordings, respectively. This indicates that, in addition to noise, regular filtering is mistakenly removing significant components of the EGM, as Figs. 7 and 8 display for several examples.

On the other hand, it is interesting to note that results for DWT- and PWT-based methods were quite similar, although both made use of different wavelet decomposition strategies.⁵⁴ Slightly better outcomes were only observed for bipolar EGMs with the DWT and for unipolar recordings with the WPT-based

approach (see Figs. 3 and 4). Moreover, the experimentally obtained optimal wavelet parameters were also greatly different in both methods, especially regarding decomposition levels and denoising thresholds. A similar behavior was also observed in most of the tested wavelet functions. This wide variety of results with respect to levels, thresholds and decomposition strategies could be justified by the fact that notably different morphologies can be found among the analyzed signals and even, sometimes, within the same signal. Nonetheless, the obtained results still confirm the high versatility of the WT. This is an important advantage, since its adaptability allows to remove efficiently noise in a wide variety of recordings, including other cardiac signals such as the ECG²⁸ and the transmembrane fluorescence optical recording from voltage-dependent dyes.⁵⁹ According to these previous works, WT-based methods have also proven here top performance in EGM waveform preservation and denoising, both under clean or very noisy conditions. To this respect, variations between the synthesized $x(n)$ and denoised $\hat{x}(n)$ signals lower than 1% were noticed under low noise conditions for the vast majority of indices related to time and frequency morphological preservation (see Figs. 3 and 4). Furthermore, the increasing presence of noise degraded WT-based method performance, but in a significantly lower amount than for regular filtering. Another interesting point was that the rate of falsely detected atrial activations from the denoised signals with these algorithms was drastically reduced even in the presence of high noise contamination. Thus, P^+ still remained around 90% for a SNR of 5 dB, while this rate decreased around 70 and 65% for regular filtering and EMD, respectively.

From the noise reduction point of view, the superior performance of WT-based methods compared with the other ones has also been demonstrated in Figs. 5, 6, 7, and 8. WT-based algorithms provided recordings with the lowest levels of noise, also preserving substantially waveform morphology, high-frequencies and abrupt atrial activations, their only drawback being a slight reduction in signal amplitude provoked by the soft thresholding.⁵¹ This alteration could explain the variations of $\Delta\rho$, ΔDF and ΔRI higher than 10% observed for very noisy cases with SNR of 5 dB in Figs. 3 and 4. Nonetheless, given the promising results obtained for values of SNR > 5 dB, the design of more advanced thresholding rules to mitigate this problem does not seem a prime issue. In any case, future works could address this topic in a similar way as with ECG denoising.⁵¹

As can also be observed in Figs. 7 and 8, the EMD-based approach resulted in a noisier signal than the WT-based algorithms. This outcome could justify the rela-

tively high variations observed between synthesized $x(n)$ and recovered $\hat{x}(n)$ recordings in most of the analyzed parameters both for unipolar and bipolar EGM recordings with values of $\text{SNR} \leq 15$ dB (see Figs. 3 and 4), thus provoking more distorted atrial activations in comparison with the WT-based methods. This poor performance could be explained by the fact that IMFs from lower levels can still contain high-frequency information from the atrial activations which is disregarded when these levels are considered as noise. Given that the present study made use of the most popular EMD-based denoising, which discards complete IMFs,¹⁰ the best trade-off between noise reduction and waveform preservation was reached by selecting $K = 2$, thus the reconstructed signal $\hat{x}(n)$ presented the noise mainly contained by $c_2(n)$ and $c_3(n)$. A similar finding has also been reported by previous works dealing with EMD-based ECG denoising, which have revealed that high-frequency IMFs contain information from the QRS complexes in addition to noise.²⁸

Finally, the increase of computational load associated to the proposed EGM denoising algorithms deserves a comment. Thus, in average for the synthesized and real EGM recordings, the computational time per sample was about 50 ns, 0.8 μ s, 5 μ s and 1 ms for regular filtering, DWT-, WPT- and EMD-based approaches, respectively. Note that both WT-based algorithms provided a notably better EGM waveform preservation than the regular approach at the cost of increasing computational load. Nonetheless, bearing in mind that computational time limitations can be easily avoided by using specific digital signal processors or complex programmable logic devices, such as FPGAs,²¹ the WT-based algorithms could be easily run in real-time under current commercial devices, which typically use a comfortable EGM sampling rate of about 1 kHz. Indeed, some recent works have proven that the DWT-based denoising of different physiological signals, even with extensive additional processing, can be successfully run online.^{11,21} Contrarily, some extra difficulties could arise in the case of EMD due to its significantly high computational load. Nonetheless, in view of its poor results compared with the WT-based methods, its integration into commercial devices does not seem to deserve much attention.

Clinical Implications

Despite the fact that regular filtering provokes significant EGM waveform alteration and poor noise reduction, such aggressive filtering between 30 and 300 Hz is currently a routine practice in electrophysiology studies.²⁶ Although previous clinical studies suggest that useful information still remains in the EGMs filtered by this approach,⁵³ undoubtedly an-

other not yet quantified amount of information is being disregarded when producing such a significantly different resulting signal. Indeed, when a signal is notably distorted, two relevant hazards occur. On the one hand, the association between altered morphological features in the resulting signal and their underlying clinical implications can be unclear. Thus, when morphological and spectral variations higher than 40 and 10%, respectively, between original and preprocessed bipolar EGMs are provoked (even for a SNR as high as 20 dB) on features such as ρ RI or DF (see Fig. 4), the clinical validity of these metrics is completely doubtful. On the other hand, when a preprocessing approach is too aggressive, interesting information from the original signal may be lost, as Figs. 7 and 8 have shown. That information may, or may not, be useful to improve clinical diagnosis or treatment of AF, but clearly it can lead to different clinical results in later stages. In fact, a less distorted signal will allow the obtention of a more realistic view about the atrial activity dynamics through different atrial mapping representations, such as voltage cartography, atrial activation maps, rotor maps or dominant frequency maps.³⁶ Hence, only when preprocessing is able to preserve the original morphology of the EGM, one can be completely sure that the obtained results are totally reliable and in accordance with reality.

Precisely, the current widespread use of the regular approach for EGM filtering could be one of the many reasons explaining inconclusive results provided by a variety of electrophysiological studies. For instance, a standardized ablation protocol for persistent AF has not been achieved yet.⁵⁸ To this respect, catheter ablation based on targeting areas with high DF has been proposed as an alternative for patients with persistent AF.^{4,48} Thus, in addition to the common pulmonary vein isolation, atrial sites showing a DF at least 20% higher than their surrounding points are targeted in this protocol.⁴ However, given the relevant differences observed between DF values obtained from the original and regularly preprocessed EGMs, it is impossible to assure that proper atrial sites are being currently ablated. This aspect may turn the validation of this protocol clinically questionable. The same comment also applies to ablation based on targeting atrial points with complex fractionated EGMs.² In this case, the presence of high levels of noise after EGM preprocessing can make the successful identification of that fractionated areas very difficult. Obviously, a completely successful ablation guided procedure is unreachable through the sole use of improved EGM preprocessing, however, this stage might be undoubtedly helpful in providing truthful signals aimed at reaching novel insights about AF mechanisms which are unknown to date.

Limitations

Only mid and high-frequency noise reduction has been detachedly analyzed in the present work. Although this is not a realistic scenario, since EGMs also present baseline wandering, power-line interference and far-field ventricular contamination, a more accurate performance assessment of the proposed denoising algorithms is achieved in this way.¹⁰ Nonetheless, given that these nuisance interferences could also be removed by using WT-based approaches,^{27,43,47} the development of an unified methodology to obtain a compact, simple and computationally light preprocessing approach both for unipolar and bipolar EGMs will be explored in future works. Similarly, other alternative denoising algorithms, such as adaptive noise cancellation, will also be assessed within this context.

CONCLUSIONS

Regular filtering applied both to unipolar and bipolar EGMs has altered substantially atrial waveform morphology and spectral properties, thus providing distorted information to later analysis as well as stages of cardiac electrophysiology systems. Moreover, it has proven reduced ability to remove moderate levels of noise. Contrarily, denoising algorithms based on Wavelet transform have shown a great capability to reduce huge levels of noise preserving EGM time morphology and spectral distribution. Hence, the use of an adequate preprocessing is recommended in routine EGM acquisition. In this way, undistorted information may provide new insights about the mechanisms triggering and maintaining AF, thus improving current understanding, management and treatment of the arrhythmia.

ELECTRONIC SUPPLEMENTARY MATERIAL

The online version of this article (doi:10.1007/s10439-017-1832-6) contains supplementary material, which is available to authorized users.

ACKNOWLEDGMENTS

This work was supported by the projects TEC2014-52250-R from the Spanish Ministry of Economy and Competitiveness and PPII-2014-026-P from Junta de Comunidades de Castilla-La Mancha.

CONFLICT OF INTEREST

The authors declare no conflict of interest.

REFERENCES

- ¹Addison, P. S. Wavelet transforms and the ECG: a review. *Physiol. Meas.* 26(5):R155–R199, 2005.
- ²Aksu, T., T. E. Guler, K. Yalin, and A. Oto. Unanswered questions in complex fractionated atrial electrogram ablation. *Pacing Clin. Electrophysiol.* 39(11):1269–1278, 2016.
- ³Alcaraz, R., F. Hornero, and J. J. Rieta. Assessment of non-invasive time and frequency atrial fibrillation organization markers with unipolar atrial electrograms. *Physiol. Meas.* 32(1):99–114, 2011.
- ⁴Atienza, F., J. Almendral, J. Jalife, S. Zlochiver, R. Ploutz-Snyder, E. G. Torrecilla, A. Arenal, J. Kalifa, F. Fernández-Avilés, and O. Berenfeld. Real-time dominant frequency mapping and ablation of dominant frequency sites in atrial fibrillation with left-to-right frequency gradients predicts long-term maintenance of sinus rhythm. *Heart Rhythm* 6(1):33–40, 2009.
- ⁵Atienza, F., J. Almendral, J. Moreno, R. Vaidyanathan, A. Talkachou, J. Kalifa, A. Arenal, J. P. Villacastín, E. G. Torrecilla, A. Sánchez, R. Ploutz-Snyder, J. Jalife, and O. Berenfeld. Activation of inward rectifier potassium channels accelerates atrial fibrillation in humans: evidence for a reentrant mechanism. *Circulation* 114(23):2434–2442, 2006.
- ⁶Blanco-Velasco, M., B. Weng, and K. E. Barner. ECG signal denoising and baseline wander correction based on the empirical mode decomposition. *Comput. Biol. Med.* 38(1):1–13, 2008.
- ⁷Boardman, A., F. S. Schindwein, A. P. Rocha, and A. Leite. A study on the optimum order of autoregressive models for heart rate variability. *Physiol. Meas.* 23(2):325–336, 2002.
- ⁸Botteron, G. W. and J. M. Smith. A technique for measurement of the extent of spatial organization of atrial activation during atrial fibrillation in the intact human heart. *IEEE Trans. Biomed. Eng.* 42(6):579–586, 1995.
- ⁹Castells, F., R. Cervigón, and J. Millet. On the preprocessing of atrial electrograms in atrial fibrillation: understanding Botteron's approach. *Pacing Clin. Electrophysiol.* 37(2):133–143, 2014.
- ¹⁰Chang, K.-M. Ensemble empirical mode decomposition for high frequency ECG noise reduction. *Biomed. Tech. (Berl.)* 55(4):193–201, 2010.
- ¹¹Chen, S.-W. and Y.-H. Chen. Hardware design and implementation of a wavelet de-noising procedure for medical signal preprocessing. *Sensors (Basel)* 15(10):26396–26414, 2015.
- ¹²Chugh, S. S., R. Havmoeller, K. Narayanan, D. Singh, M. Rienstra, E. J. Benjamin, R. F. Gillum, Y.-H. Kim, J. H. McAnulty, Jr, Z.-J. Zheng, M. H. Forouzanfar, M. Naghavi, G. A. Mensah, M. Ezzati, and C. J. L. Murray. Worldwide epidemiology of atrial fibrillation: a Global Burden of Disease 2010 Study. *Circulation* 129(8):837–847, 2014.
- ¹³Ciaccio, E. J., A. B. Biviano, and H. Garan. Computational method for high resolution spectral analysis of fractionated atrial electrograms. *Comput. Biol. Med.* 43(10):1573–1582, 2013.
- ¹⁴Corino, V. D. A., M. W. Rivolta, R. Sassi, F. Lombardi, and L. T. Mainardi. Ventricular activity cancellation in electrograms during atrial fibrillation with constraints on residuals' power. *Med. Eng. Phys.* 35(12):1770–1777, 2013.
- ¹⁵de Bakker, J. M. T. and F. H. M. Wittkamp. The pathophysiologic basis of fractionated and complex electrograms and the impact of recording techniques on their

- detection and interpretation. *Circ. Arrhythm. Electrophysiol.* 3(2):204–213, 2010.
- ¹⁶Donoho, D. and I. Johnstone. Ideal spatial adaptation by wavelet shrinkage. *Biometrika* 81:425–455, 1994.
- ¹⁷Donoho, D. and I. Johnstone. Adapting to unknown smoothness via wavelet shrinkage. *J. Am. Stat. Assoc.* 90:1200–1224, 1995.
- ¹⁸Everett, IV, T. H., L. C. Kok, R. H. Vaughn, J. R. Moorman, and D. E. Haines. Frequency domain algorithm for quantifying atrial fibrillation organization to increase defibrillation efficacy. *IEEE Trans. Biomed. Eng.* 48(9): 969–978, 2001.
- ¹⁹Faes, L., G. Nollo, R. Antolini, F. Gaita, and F. Ravelli. A method for quantifying atrial fibrillation organization based on wave-morphology similarity. *IEEE Trans. Biomed. Eng.* 49(12 Pt 2):1504–1513, 2002.
- ²⁰Flandrin, P., G. Rilling, and P. Goncalves. Empirical mode decomposition as a filter bank. *IEE Signal Process. Lett.* 11:112–114, 2004.
- ²¹Gutiérrez-Gnecchi, J. A., R. Morfin-Magana, D. Lorias-Espinoza, A. C. Tellez-Anguiano, E. Reyes-Archundia, A. Méndez-Patino, and R. Castaneda-Miranda. DSP-based arrhythmia classification using wavelet transform and probabilistic neural network. *Biomed. Signal Process. Control* 32:44–56, 2017.
- ²²Haïssaguerre, M., M. Hocini, A. Denis, A. J. Shah, Y. Komatsu, S. Yamashita, M. Daly, S. Amraoui, S. Zellerhoff, M.-Q. Picat, A. Quotb, L. Jesel, H. Lim, S. Ploux, P. Bordachar, G. Attuel, V. Meillet, P. Ritter, N. Derval, F. Sacher, O. Bernus, H. Cochet, P. Jaïs, and R. Dubois. Driver domains in persistent atrial fibrillation. *Circulation* 130(7):530–538, 2014.
- ²³Heijman, J., V. Algalarrondo, N. Voigt, J. Melka, X. H. T. Wehrens, D. Dobrev, and S. Nattel. The value of basic research insights into atrial fibrillation mechanisms as a guide to therapeutic innovation: a critical analysis. *Cardiovasc. Res.* 109(4):467–479, 2016.
- ²⁴Houben, R. P. M. and M. A. Allesie. Processing of intracardiac electrograms in atrial fibrillation. Diagnosis of electropathological substrate of AF. *IEEE Eng. Med. Biol. Mag.* 25(6):40–51, 2006.
- ²⁵Huang, N. E., Z. Shen, S. R. Long, M. C. Wu, H. H. Shih, Q. Zheng, N.-C. Yen, C. C. Tung, and H. H. Liu. The empirical mode decomposition and the Hilbert spectrum for nonlinear and non-stationary time series analysis. *Proc. R. Soc. Lond. A* 454:903–995, 1998.
- ²⁶Issa, Z. F., J. W. Miller, and D. P. Zipes. *Clinical Arrhythmology and Electrophysiology: A Comparison to Braunwald's Heart Disease*, 2nd ed. Amsterdam: Elsevier, 2012.
- ²⁷Jenkal, W., R. Latif, A. Toumanari, et al. An efficient algorithm of ECG signal denoising using the adaptive dual threshold filter and the discrete wavelet transform. *Biocybern. Biomed. Eng.* 36(3):499–508, 2016.
- ²⁸Kabir, M. A. and C. Shahnaz. Denoising ECG signals based on noise reduction algorithms in EMD and wavelet domains. *Biomed. Signal Process. Control* 7:481–489, 2012.
- ²⁹Koutalas, E., S. Rolf, B. Dinov, S. Richter, A. Arya, A. Bollmann, G. Hindricks, and P. Sommer. Contemporary mapping techniques of complex cardiac arrhythmias—identifying and modifying the arrhythmogenic substrate. *Arrhythm. Electrophysiol. Rev.* 4(1):19–27, 2015.
- ³⁰Lahmiri, S. Comparative study of ECG signal denoising by wavelet thresholding in empirical and variational mode decomposition domains. *Healthc. Technol. Lett.* 1(3):104–109, 2014.
- ³¹Lian, J., G. Garner, D. Muessing, and V. Lang. A simple method to quantify the morphological similarity between signals. *Signal Process.* 90:684–688, 2010.
- ³²Liang, H., Q.-H. Lin, and J. D. Z. Chen. Application of the empirical mode decomposition to the analysis of esophageal manometric data in gastroesophageal reflux disease. *IEEE Trans. Biomed. Eng.* 52(10):1692–1701, 2005.
- ³³Luo, S. and P. Johnston. A review of electrocardiogram filtering. *J. Electrocardiol.* 43(6):486–496, 2010.
- ³⁴Mallat, S. *A Wavelet Tour of Signal Processing*. Burlington: Academic Press, 1999.
- ³⁵Narayan, S. M. and J. A. B. Zaman. Mechanistically based mapping of human cardiac fibrillation. *J. Physiol.* 594(9):2399–2415, 2016.
- ³⁶Nedios, S., P. Sommer, A. Bollmann, and G. Hindricks. Advanced mapping systems to guide atrial fibrillation ablation: electrical information that matters. *J. Atr. Fibrillation* 8(6):1337, 2016.
- ³⁷Ng, J., A. I. Borodyanskiy, E. T. Chang, R. Villuendas, S. Dibs, A. H. Kadish, and J. J. Goldberger. Measuring the complexity of atrial fibrillation electrograms. *J. Cardiovasc. Electrophysiol.* 21(6):649–655, 2010.
- ³⁸Ng, J. and J. J. Goldberger, eds. *Intracardiac electrograms. In Practical Signal and Image Processing in Clinical Cardiology*. London: Springer, 2010, pp. 319–348.
- ³⁹Ng, J., A. H. Kadish, and J. J. Goldberger. Technical considerations for dominant frequency analysis. *J. Cardiovasc. Electrophysiol.* 18(7):757–764, 2007.
- ⁴⁰Ng, J., V. Sehgal, J. K. Ng, D. Gordon, and J. J. Goldberger. Iterative method to detect atrial activations and measure cycle length from electrograms during atrial fibrillation. *IEEE Trans. Biomed. Eng.* 61(2):273–278, 2014.
- ⁴¹Nollo, G., M. Marconcini, L. Faes, F. Bovo, F. Ravelli, and L. Bruzzzone. An automatic system for the analysis and classification of human atrial fibrillation patterns from intracardiac electrograms. *IEEE Trans. Biomed. Eng.* 55(9):2275–2285, 2008.
- ⁴²Oesterlein, T. G., G. Lenis, D.-T. Rudolph, A. Luik, B. Verma, C. Schmitt, and O. Dössel. Removing ventricular far-field signals in intracardiac electrograms during stable atrial tachycardia using the periodic component analysis. *J. Electrocardiol.* 48(2):171–180, 2015.
- ⁴³Poornachandra, S. and N. Kumaravel. A novel method for the elimination of power line frequency in ECG signal using hyper shrinkage function. *Digital Signal Process.* 18(2):116–126, 2008.
- ⁴⁴Potter, B. J. and J. Le Lorier. Taking the pulse of atrial fibrillation. *Lancet* 386(9989):113–115, 2015.
- ⁴⁵Rafiee, J., M. A. Rafiee, N. Prause, and M. P. Schoen. Wavelet basis functions in biomedical signal processing. *Expert Syst. Biomed. Signal Process.* 38:6190–6201, 2011.
- ⁴⁶Ravelli, F., M. Masè, A. Cristoforetti, M. Marini, and M. Disertori. The logical operator map identifies novel candidate markers for critical sites in patients with atrial fibrillation. *Prog. Biophys. Mol. Biol.* 115(2–3):186–197, 2014.
- ⁴⁷Sanchez, C., J. J. Rieta, F. Castells, J. Ródenas, and J. Millet. Atrial activity extraction in Holter registers using adaptive Wavelet analysis. *Annual International Conference of Computers in Cardiology*, vol. 30, pp. 569–572, 2003.
- ⁴⁸Sanders, P., O. Berenfeld, M. Hocini, P. Jaïs, R. Vaidyanathan, L.-F. Hsu, S. Garrigue, Y. Takahashi, M. Rotter, F. Sacher, C. Scavée, R. Ploutz-Snyder, J. Jalife, and M. Haïssaguerre. Spectral analysis identifies sites of high-frequency activity maintaining atrial fibrillation in humans. *Circulation* 112(6):789–797, 2005.

- ⁴⁹Schnabel, R. B., X. Yin, P. Gona, M. G. Larson, A. S. Beiser, D. D. McManus, C. Newton-Cheh, S. A. Lubitz, J. W. Magnani, P. T. Ellinor, S. Seshadri, P. A. Wolf, R. S. Vasan, E. J. Benjamin, and D. Levy. 50 year trends in atrial fibrillation prevalence, incidence, risk factors, and mortality in the Framingham Heart Study: a cohort study. *Lancet* 386(9989):154–162, 2015.
- ⁵⁰Schotten, U., D. Dobrev, P. G. Platonov, H. Kottkamp, and G. Hindricks. Current controversies in determining the main mechanisms of atrial fibrillation. *J. Intern. Med.* 279(5):428–438, 2016.
- ⁵¹Singh, B. N. and A. K. Tiwari. Optimal selection of wavelet basis function applied to ECG signal denoising. *Digital Signal Process.* 16:275–287, 2006.
- ⁵²Smital, L., M. Vitek, J. Kozumplík, and I. Provazník. Adaptive wavelet Wiener filtering of ECG signals. *IEEE Trans. Biomed. Eng.* 60(2):437–445, 2013.
- ⁵³Stevenson, W. G. and K. Soejima. Recording techniques for clinical electrophysiology. *J. Cardiovasc. Electrophysiol.* 16(9):1017–1022, 2005.
- ⁵⁴Tikkanen, P. E. Nonlinear wavelet and wavelet packet denoising of electrocardiogram signal. *Biol. Cybern.* 80(4):259–267, 1999.
- ⁵⁵Venkatachalam, K. L., J. E. Herbrandson, and S. J. Asirvatham. Signals and signal processing for the electrophysiologist. Part I: electrogram acquisition. *Circ. Arrhythm. Electrophysiol.* 4(6):965–973, 2011.
- ⁵⁶Venkatachalam, K. L., J. E. Herbrandson, and S. J. Asirvatham. Signals and signal processing for the electrophysiologist. Part II: signal processing and artifact. *Circ. Arrhythm. Electrophysiol.* 4(6):974–981, 2011.
- ⁵⁷Wodchis, W. P., R. S. Bhatia, K. Leblanc, N. Meshkat, and D. Morra. A review of the cost of atrial fibrillation. *Value Health* 15(2):240–248, 2012.
- ⁵⁸Wynn, G. J., M. Das, L. J. Bonnett, S. Panikker, T. Wong, and D. Gupta. Efficacy of catheter ablation for persistent atrial fibrillation: a systematic review and meta-analysis of evidence from randomized and nonrandomized controlled trials. *Circ. Arrhythm. Electrophysiol.* 7(5):841–852, 2014.
- ⁵⁹Xiong, F., X. Qi, S. Nattel, and P. Comtois. Wavelet analysis of cardiac optical mapping data. *Comput. Biol. Med.* 65:243–255, 2015.
- ⁶⁰Zoni-Berisso, M., F. Lercari, T. Carazza, and S. Domenicucci. Epidemiology of atrial fibrillation: European perspective. *Clin. Epidemiol.* 6:213–220, 2014.